AFRL-SN-RS-TR-1998-23
Final Technical Report
March 1998

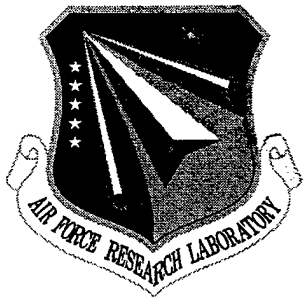

SPECTRAL HOLOGRAPHY USING BULK PHOTO-REFRACTIVE CRYSTALS FOR HIGH-SPEED LIGHTWAVE PROCESSING

Purdue Research Foundation

APPROVED FOR PUBLIC RELEASE; DISTRIBUTION UNLIMITED.

AIR FORCE RESEARCH LABORATORY
SENSORS DIRECTORATE
ROME RESEARCH SITE
ROME, NEW YORK

This report has been reviewed by the Air Force Research Laboratory, Information Directorate, Public Affairs Office (IFOIPA) and is releasable to the National Technical Information Service (NTIS). At NTIS it will be releasable to the general public, including foreign nations.

AFRL-SN-RS-TR-1998-23 has been reviewed and is approved for publication.

APPROVED: George A. Brost

GEORGE A. BROST
Project Engineer

FOR THE DIRECTOR: Robert G. Polce

ROBERT G. POLCE, Acting Chief
Rome Operations Office
Sensors Directorate

If your address has changed or if you wish to be removed from the Air Force Research Laboratory Rome Research Site mailing list, or if the addressee is no longer employed by your organization, please notify AFRL/SNDR, 25 Electronic Pky, Rome, NY 13441-4515. This will assist us in maintaining a current mailing list.

Do not return copies of this report unless contractual obligations or notices on a specific document require that it be returned.

REPORT DOCUMENTATION PAGE

Form Approved
OMB No. 0704-0188

1. AGENCY USE ONLY *(Leave blank)*	2. REPORT DATE	3. REPORT TYPE AND DATES COVERED
	March 1998	**FINAL Jun 96 – Jun 97**

4. TITLE AND SUBTITLE
SPECTRAL HOLOGRAPHY USING BULK PHOTOREFRACTIVE CRYSTALS FOR HIGH-SPEED LIGHTWAVE PROCESSING

5. FUNDING NUMBERS
C - F30602-96-2-0114
PE - 62702F
PR - 4600
TA - P5
WU - PG

6. AUTHOR(S)
Andrew M. Weiner, David D. Nolte

7. PERFORMING ORGANIZATION NAME(S) AND ADDRESS(ES)
Purdue Research Foundation
1063 Hovde Hall
West Lafayette IN 47907

8. PERFORMING ORGANIZATION REPORT NUMBER

9. SPONSORING / MONITORING AGENCY NAME(S) AND ADDRESS(ES)
Air Force Research Laboratory/SNDR
25 Electronic Pky
Rome NY 13441-4515

10. SPONSORING / MONITORING AGENCY REPORT NUMBER
AFRL-SN-RS-TR-1998-23

11. SUPPLEMENTARY NOTES
Rome Laboratory Project Engineer: George A. Brost, SNDR, (315) 330-7669

12a. DISTRIBUTION AVAILABILITY STATEMENT
APPROVED FOR PUBLIC RELEASE; DISTRIBUTION UNLIMITED

12b. DISTRIBUTION CODE

13. ABSTRACT *(Maximum 200 words)*
The ultimate objective of this project is to assess the use of bulk photorefractive crystals in a femtosecond spectral holography setup to control and shape femtosecond pulses. By recording a hologram using near-infrared light for which the crystals have high sensitivity, and reading out the holograms using 1.5 μm light, it should be possible to generate shaped pulses sequences at the 1.5 μm wavelength important for high speed fiber communications. One potential difficulty with this approach is the limited optical bandwidth expected for readout of a hologram recorded using a different wavelength, which could limit the minimum pulse duration accessible using this approach. We have performed a theoretical and experimental investigation of the optical bandwidth of bulk holograms read out using broadband femtosecond pulses. Experiments performed using a bulk InP:Fe photorefractive crystal verify the theoretically predicted variation of bandwidth with holographic grating period. Our experiments show that by using a grating period of 10 μm, more than enough bandwidth is available for processing of 100 femtosecond pulses. These results confirm the viability of the proposed pulse shaping approach based on bulk holographic media inside a spectral holography apparatus.

14. SUBJECT TERMS	15. NUMBER OF PAGES
photorefraction, spectral holography, lightwave processing	28
	16. PRICE CODE

17. SECURITY CLASSIFICATION OF REPORT	18. SECURITY CLASSIFICATION OF THIS PAGE	19. SECURITY CLASSIFICATION OF ABSTRACT	20. LIMITATION OF ABSTRACT
UNCLASSIFIED	**UNCLASSIFIED**	**UNCLASSIFIED**	**UNLIMITED**

NSN 7540-01-280-5500

Standard Form 298 (Rev. 2-89)
Prescribed by ANSI Std. Z39-18

TABLE OF CONTENTS

1. Introduction

The development and the commercial availability of sub-100 femtosecond lasers open up possibilities to extend the bandwidth of optical communications and signal processing into the THz range. Fourier filtering in a femtosecond pulse shaper[1] is one of the important techniques for processing optical signals in the Fourier domain. Among many filtering masks for femtosecond pulses, such as fixed amplitude and phase masks[1], liquid crystal spatial light modulators[2] and acousto-optical modulators[3], dynamic holograms are interesting because of their flexibility and possibility in implementing dynamic processing[4]. Photorefractive materials[5] are prominent dynamic holographic media because of their low intensity requirement for writing and large refractive index changes. Among photorefractive materials, ferroelectric crystals such as $BaTiO_3$, $LiNbO_3$ and $KNbO_3$ have large electro-optic coefficients, leading to a strong photorefractivity but with a slow grating response of seconds. For using photorefractive materials to process femtosecond pulses in the frequency domain, a sufficient large space-bandwidth product is required. Due to the strong Bragg selectivity, volume holograms in photorefractive crystals are excellent for high-capacity holographic data storage[6], but they are considered as unsuitable for implementing Fourier-plane filtering operations in space-domain image processing[7]. When volume holograms are written and readout by lasers with greatly different wavelengths, holographic memories also experience limitations in storage density due to the Bragg selectivity, although this is not a problem for identical write and readout wavelengths[8]. Another application of volume holography, of interest to us here, is to use the volume hologram for spatial patterning of spatially dispersed frequency components within a femtosecond pulse shaping apparatus. We are particularly interested in the possibility of writing at relatively short wavelengths where photorefractive crystals have good sensitivity and reading out at larger wavelengths. This could be applied to implement holographic pulse shaping of 1.5 μm optical pulses in the optical communications band. A key issue for this scheme is whether the volume hologram, written by a cw laser producing a constant hologram

period, will have a sufficient Bragg matching bandwidth to diffract the entire spectrum of a femtosecond pulse. Our goal in this work is to investigate the bandwidth of femtosecond pulses diffracted from volume holograms. Our results elucidate the conditions under which sufficient bandwidth is available to diffract the entire bandwidths of femtosecond pulses.

In previous experiments $LiNbO_3$ was used for processing femtosecond pulses in the frequency domain[9], but due to the concern of Bragg-limitation, a short crystal (1 mm) and small incident angles were used, which would strongly reduce the diffraction efficiency in this material. Thin holograms such as GaAlAs/GaAs multiple quantum wells, where the Bragg-limitation is eliminated because the diffraction is in the Raman-Nath regime, were used for femtosecond pulse manipulation[10] with the response time improved from seconds in $LiNbO_3$ to microseconds. But the diffraction efficiency is still limited by the short interaction length. For volume holograms with large interaction length, the Bragg selection becomes weaker when the incident angle is small, i.e. if the grating spacing is large. For photorefractive oxides, unfortunately, due to the diffusion limitation, the optimum grating spacing for diffraction is quite small, typically ≤ 1 μm. On the other hand, photorefractive semiconductors such as GaAs, InP and CdTe have much faster response time, because of their large charge mobility. The weaker photorefractivity due to the small electro-optic coefficients in such materials can be enhanced by applying an external electric field. As a result, the charge drift becomes the dominant transport mechanism, which moves the optimum gratings spacing to a larger value, usually ≥ 10 μm, where the Bragg-selectivity becomes weaker. In addition, photorefractive semiconductors are sensitive in the near-infrared wavelengths for optical communications. All these may make the photorefractive semiconductor crystals suitable for femtosecond applications using Fourier-plane filtering. We use photorefractive InP:Fe as the holographic material, because it has been demonstrated to be a prominent photorefractive semiconductor with high two-wave mixing gain[11,12]. Photorefractive phenomena requiring high beam coupling strength, such as self-pumped phase conjugation[13], double pumped and double

color pumped phase conjugate mirror[14], were observed in InP:Fe at different wavelengths. In this work we investigate diffraction of femtosecond pulses from volume holograms in InP:Fe both theoretically and experimentally. We demonstrate a diffraction bandwidth of tens of nanometers around 1.5 μm for a 7.8 mm thick InP:Fe crystal, which is more than sufficient to accommodate the entire bandwidth of a 100 fsec pulse. This result suggests that InP:Fe can be a suitable material for femtosecond pulse processing at 1.5 μm using volume holography within a femtosecond pulse shaper.

2. Theoretical consideration

In this section, we start with the coupled wave theory by Kogelnik[15] and discuss the diffraction of the diffraction of a broad-band femtosecond pulse from a volume hologram in a photorefractive crystal, which is written by two copolarized cw pump beams at a wavelength of λ_p in the air. As shown in Fig. 1 the two beams enter the surface of the photorefractive material at the same angle θ'_p (the angle inside the crystal is θ_p). The photorefractive grating has the form: $\Delta n = \Delta n_0 \cos(Kx)$, where Δn_0 is the maximum refractive index change and $K = 2\pi/\Lambda$ is the grating vector length with the grating spacing $\Lambda = \lambda_p/2\sin\theta'_p$. The reading beam $E_r = E_r(z)e^{-i\vec{k}\cdot\vec{r}}$, here the broadband femtosecond optical pulses with a center wavelength of λ_r, enters the crystal at an angle of θ'_r (the angle inside the crystal is θ_r). It is diffracted by the refractive index grating. When the diffraction efficiency is low, we can assume that the reading beam itself is little perturbed in the process and the coupled wave equations can be reduced to the following form:

$$\cos\theta_r \frac{dE_d(z)}{dz} - i\frac{K^2\Delta\lambda}{2\pi n_r}E_d(z) = -i\kappa E_r \qquad (1)$$

where E_r and $E_d(z)$ are the electric fields of the reading and diffracted beams respectively, $\kappa = \pi\Delta n_r/2\lambda_r$ is the coupling coefficient with the amplitude of the refractive index modulation Δn_r,

and $\Delta\lambda = \lambda - \lambda_r$. Here we assume that the θ_r equals the Bragg angle for the center wavelength λ_r. The analytical solution for the diffracted field is then

$$E_d(z) = 2iE_r \frac{4\pi n_r \kappa}{K^2 \Delta\lambda} \exp\left(i \frac{K^2 \Delta\lambda}{8\pi n_r \cos\theta_r} z\right) \sin\left(\frac{K^2 \Delta\lambda}{8\pi n_r \cos\theta_r} z\right) \tag{2}$$

The diffraction efficiency is defined as $\eta = E_d E_d^* / E_r E_r^*$. The wavevector of the diffracted beam is specified by the relation: $\vec{k}_d = \vec{k}_r - \vec{K}$, and when Bragg condition is satisfied for a specific wavelength, for example, the center wavelength λ_r (i.e. $\Delta\lambda = 0$), we have $2k_r \cdot \sin\theta_r = K = 2k_p \cdot \sin\theta_p$ with $k_d = k_r$, and the maximum efficiency is achieved

$$\eta_0 = \left(\frac{\kappa}{\cos\theta_r} d\right)^2, \tag{3}$$

where d is the thickness of the crystal. For the broadband reading beam at the same incident angle, apparently it is impossible to let all wavelength components satisfy the Bragg condition at the same time. At wavelengths different from λ_r, the diffraction efficiency will decrease. The normalized efficiency has the form

$$\frac{\eta}{\eta_0} = \text{sinc}^2\left(\frac{K^2 \Delta\lambda d}{8\pi n_r \cos\theta_r}\right) = \text{sinc}^2\left(\frac{\pi \Delta\lambda d}{2\Lambda^2 n_r \cos\theta_r}\right). \tag{4}$$

From Eq. 4, we can find a wavelength range $2\Delta\lambda_{1/2}$, beyond which the diffraction will drop blow 50%:

$$\Delta\lambda_{1/2} = 0.886 \frac{\Lambda^2 n_r \cos\theta_r}{d}. \tag{5}$$

We see that the bandwidth is inversely proportional to the grating thickness d, so that traditionally it is believed that thick crystals are unsuitable for broadband applications. However it

is also observed that, $\Delta\lambda_{1/2}$ nearly depends on the square of the grating period, when the changes in the term of $\cos\theta_r$ can be overlooked(which is true at small incident angle). By increasing the grating period, it is then likely to achieve a large bandwidth. As we will show in the later sections, our results verify this experimentally. On the other hand, the diffraction efficiency from eq. (3) is independent of grating period, again assuming small angles where $\cos(\theta_r)$ remains near unity. Therefore, one expects to be able to achieve high diffraction bandwidth without sacrificing diffraction efficiency.

For the case with a finite incident spectrum $|E_{IN}(\lambda)|^2$, by using Eq. 4, which, under low conversion efficiency condition, matches very well with the results given in [14], the output spectrum $|E_{OUT}(\lambda)|^2$ is given by

$$|E_{out}(\lambda)|^2 = \left(\frac{\kappa}{\cos\theta_r} d\right)^2 \mathrm{sinc}^2\left(\frac{\pi\Delta\lambda d}{2\Lambda^2 n_r \cos\theta_r}\right) |E_{IN}(\lambda)|^2, \qquad (6)$$

which is used to calculate the diffraction output bandwidth and spectrum under our experimental situation. The simulation results and the comparison with experimental data are given in the following sections.

3. Experimental setup

The experimental setup is shown in Fig. 1, which is a non-degenerate four-wave mixing geometry. The two holograms writing beams are from a cw diode laser at a wavelength of 980 nm with s-polarization. The femtosecond probe beam with a pulse width of 150 fs at 1550 nm is from a optical parameter oscillator (OPO), pumped by mode-locked Ti:Sapphire laser. The holographic medium is a holographically cut photorefractive InP:Fe crystal with a dimension of 4.2x5.0x7.8 mm^3, provided by G. A. Brost at Rome Laboratory. The polarization of the read-out beam is kept

to be also s-polarized to obtain the maximum diffraction for this crystal orientation[16]. An electric field is applied along the <001> direction across the 4.2 mm distance with silver paint as electrodes. The optical surfaces are the (110) planes with an interaction length of 7.8 mm. The absorption coefficient at 980 nm is 5.2 cm^{-1}, and the refractive index is about 3.327 and 3.134 at the pump and reading wavelengths respectively. The intersection angle $2\theta'_p$ of the two writing beams can be changed to obtain different grating spacings. In order to exploit the intensity-temperature resonance in InP:Fe, which leads to a strong refractive index change[17], the crystal is temperature controlled by a thermoelectric cooler. The femtosecond probe beam enters the crystal at the Bragg angle. The diffracted intensity and spectrum are detected by a photodiode and an optical spectrum analyzer (OSA).

4. Results and Discussion

Before the femtosecond probe beam is sent to the crystal for diffraction experiment, the hologram written in the InP:Fe crystal at 980 nm is characterized and optimized by a two-beam coupling experiment, where the energy exchange between the two writing beams is measured. The two-beam coupling gain coefficient Γ is defined as

$$\Gamma = \frac{1}{d} \ln\left(\frac{\beta r}{1+\beta-r}\right) \tag{7}$$

with the beam ratio β and the two-beam coupling gain r = (I_1 with I_2) /(I_1 without I_2). In order to get an optimum gain, the beam path of the two beams must be aligned to be equal. Due to the multiple longitudinal mode character and the short cavity length of the diode write laser, the coherence function is more complicated than that of conventional gas lasers and consists of a series of peaks. Fig. 2 shows the two-beam coupling gain as a function of the delay of one beam. The FWHM of the curve is just 1.3 mm. Therefore, the delay between the two writing beams must be set to a precision of a few hundred microns for our diffraction experiments.

In InP:Fe, the dominant photocarriers are holes whereas the thermally excited charges are dominantly electrons. The maximum refractive index modulation is obtained, when the dc part in the spatially modulated photocarriers is balanced by the thermally excited charges (electrons). This is called intensity-temperature resonance[16]. For our experiment at an applied field of 6 kV/cm the optimum two-beam coupling gain at an intensity of 60 mW/cm^2 is obtained at the sample temperature of 10 °C, with a value of 0.48 cm^{-1} for equal incident intensities of the two beams. Using the relation between the two-beam coupling coefficient and the refractive index change in the crystal $\Gamma = \frac{4\pi}{\lambda_p}\Delta n$, we can estimate the refractive index change to be $\Delta n \sim 4 \times 10^{-6}$, assuming a $\pi/2$ phase shift between the refractive index grating and the intensity grating, which is true under the intensity-temperature resonance[16]. It is not the intention of this paper to achieve high two-beam coupling gain. The small gain value here is mostly because of the large absorption at the 980 nm pump wavelength, which leads to a strong decrease of intensity in the crystal. As a result, the intensity-temperature resonance can not be kept along the crystal for a uniform sample temperature. At longer wavelengths, for example at 1.06 μm, the gain coefficient can be increased by at least an order of magnitude[11].

For the diffraction experiment, the femtosecond probe beams is sent to the hologram at the Bragg angle. The measured diffraction efficiency is about 10^{-3}, which agrees with the value estimated from Δn in the two-beam coupling experiment. As the femtosecond pulse with a bandwidth of 16 nm enters the crystal, the diffracted spectrum will be narrowed by the Bragg selectivity. Fig. 3 shows the diffraction spectrum from holograms with grating spacings of 4.1 and 13.9 μm, corresponding to a grating writing angles of 6.9 and 2.0 degrees, respectively. The FWHM of the diffraction spectrum at the grating spacing of 4.1 μm has a value of 8 nm, which is the half of that of the incident spectrum, whereas the value at 13.9 μm is 16 nm, equal to the input one. An experiment was also performed with a 7.3 μm grating period, where an output bandwidth of 11 nm was observed. Numerical calculations using the Kogelnik theory for these grating

spacings are also given in the figure, which agree well with the experimental data. The spectrum of the input pulse is also plotted in the figure as comparison.

Fig. 4 shows the theoretical calculation of the bandwidth of the diffracted pulse as a function of the grating spacing with a crystal length ranging from 4 to 11 mm, assuming as before an input pulse with 16 nm bandwidth. We can see that at grating spacings larger than 10 μm, the whole bandwidth of 16 nm can be reconstructed, even for the 11 mm thick crystal. The crystal thickness is an important parameter in addition to the grating spacing for determining if a hologram is in the thick or thin grating regime using the Q factor[18]

$$Q = \frac{2\pi d\lambda_r}{\Lambda^2 n_r}. \tag{8}$$

In the case of $\Lambda = 4.1$ μm, we have $Q \approx 1400$ for the 7.8 mm thick crystal. This Q-value is much larger than 1, indicating that the grating is a thick grating with an angle selectivity of $2\Delta\theta_r \approx \Lambda/d = 0.03$ degrees[14]. At $\Lambda = 14$ μm, these values become $Q \approx 117$ and $2\Delta\theta_r \approx 0.1$ degree. Although the grating is still in the thick grating regime under the definition in Eq. (8), the bandwidth of the grating diffraction is already so large, that the full spectrum of a 100 fs pulse can be reconstructed in the hologram read-out. Fig. 5 shows the possible output bandwidth as a function of the grating spacing with the input with infinity bandwidth for a crystal length of 7.8 mm. A pulse with a bandwidth of as large as 140 nm can be obtained from the diffraction at a grating spacing of 14 μm, which is an appropriate grating spacing for a strong hologram in photorefractive semiconductor with an applied electric field. As a result, photorefractive holograms can be used for applications of Fourier manipulation in the frequency domain, such as pulse shaping and processing. In contrast, the excellent angle selectivity of a thick hologram makes it unsuitable for Fourier manipulation of space-domain images.

5. Conclusions

In conclusion, we performed measurements of diffraction using femtosecond 1.5 μm pulses from gratings written by 980 nm cw light into a bulk InP:Fe crystal. We have shown that although the Bragg-selectivity is quite strong in the space domain, leading to the unsuitability of volume hologram in Fourier-filtering application like image processing, the bandwidth in the frequency domain is still large enough for the bandwidth of sub-100 fs laser pulses of tens of nanometers under certain grating conditions, such as a large grating spacing. Our experiments support the viability of using bulk InP:Fe photorefractive crystals for Fourier filtering within a pulse shaping apparatus for pulses as short as 100 fsec.

Figure captions

Fig. 1 Experimental setup for diffraction of femtosecond pulses at 1.5 μm from hologram written in photorefractive crystal at 980 nm.

Fig. 2 Two-beam coupling gain as a function of the delay of one beam. The FWHM of the main peak is 1.3 mm.

Fig. 3 Experimental diffraction spectra from the hologram with a grating spacing of a) 4.1 μm and b) 13.9 μm (solid lines). The theoretical calculations at these grating spacings (dashed lines) and the spectrum of the incident pulse (dot lines) are also given as comparison.

Fig. 4 Bandwidth of the diffracted pulse as a function of the grating spacing with a crystal length of 4, 7.8 and 11 mm, respectively. The input bandwidth is 16 nm.

Fig. 5 Output bandwidth as a function of the grating spacing with the input with infinity bandwidth in comparison with the case with 16 nm input bandwidth for a 7.8 mm long crystal, showing large potential bandwidths at large grating spacings for frequency filtering applications.

[1] A. M. Weiner, J. P. Heritage, and E. M. Kirschner, "High resolution femtosecond pulse shaping," J. Opt. Soc. Am. **B5**, 1563 (1988)

[2] A. M. Weiner, D. E. Leaird, J. S. Patel and J. R. Wullert II, "Programmable shaping of femtosecond optical pulses by use of a 128-element liquid crystal phase modulator," IEEE J. Quantum Electron. 28, 908 (1992)

[3] C. Hillegas, J. X. Tull, D. Goswami, D. Strickland, and W. S. Warren, "Femtosecond laser pulse shaping by use of microsecond radio-frequency pulses," Opt. Lett. 19, 737 (1994)

[4] K. Ema, "Real-time ultrashort pulse shaping and pulse shape measurement using a dynamic grating," Jpn. J. Appl. Phys. 30, L2046 (1991)

[5] P. Günter, J. P. Huignard, *Photorefractive Materials and Their Applications, I, II*, (Springer-Verlag, Berlin, 1988, 1989)

[6] J. Heanue, M. Bashaw, and L. Hesselink, "Optical memories implemented with photorefractive media," Opt. and Quantum Electron. 25, S611 (1993)

[7] R. A. Athale and K. Raj, "Fourier-plane filtering by a thick grating: a space-bandwidth analysis," Opt. Lett. 17, 880 (1992)

[8] J. F. Heanue, M. C. Bashaw, and L. Hesselink, "Volume holographic storage and retrieval of digital data," Science 265, 749 (1994)

[9] P. C. Sun, Y. T. Mazurenko, W. S. C. Chang, P. K. L. Yu, and Y. Fainman, "All-optical parallel-to-serial conversion by holographic spatial-to-temporal frequency encoding," Opt. Lett. 20, 1728 (1995)

[10] Y. Ding, R. M. Brubaker, D. D. Nolte, M. R. Melloch, and A. M. Weiner, "Femtosecond pulse shaping by dynamic holograms in photorefractive multiple quantum wells", Opt. Lett. 22, 718 (1997)

[11] J. E. Millerd, S. D. Koehler, E. M. Garmire, A. Partovi and A. M. Glass, "Photorefractive gain enhancement using band-edge resonance and temperature stabilization", Appl. Phys. Lett. 57, 2776 (1990)

[12] H. J. Eichler, Y. Ding, and B. Smandek: *"Two-wave mixing in InP:Fe at 1064 nm by linear and quadratic photorefractive effect"*, Opt. Commun. 94, 127-132 (1992).

[13] Y. Ding: *"Photorefractive phase conjugation in InP:Fe"*, Proc. International Conference on LASERS '94, pp. 373-376, Dec. 12-16, 1994, Quebec, Canada.

[14] N. Wolffer, P. Gravey, G. Picoli, and V. Vieux, "Double phase conjugated mirror and double color pumped oscillator using band-edge photorefractivity in InP:Fe", Opt. Commun. 89, 17 (1992)

[15] H. Kogelnik, "Coupled wave theory for thick hologram gratings," The Bell Sys. Tech. J. 48, 2909 (1969)

[16] Y. Ding, and H. J. Eichler: "Crystal orientation dependence of the photorefractive four-wave mixing in compound semiconductors of symmetry group ", Opt. Commun. 110, 456-464 (1994).

[17] G. Picoli, P. Gravey, C. Ozkul, and V. Vieux, "Theory of two-wave mixing gain enhancement in photorefractive InP:Fe: A new mechanism of resonance", J. Appl. Phys. 66, 3789 (1989).

[18] H. J. Eichler, P. Günter, D. W. Wohl, *Laser-induced dynamic gratings*, Springer-Verlag, Berlin, Germany, 1986

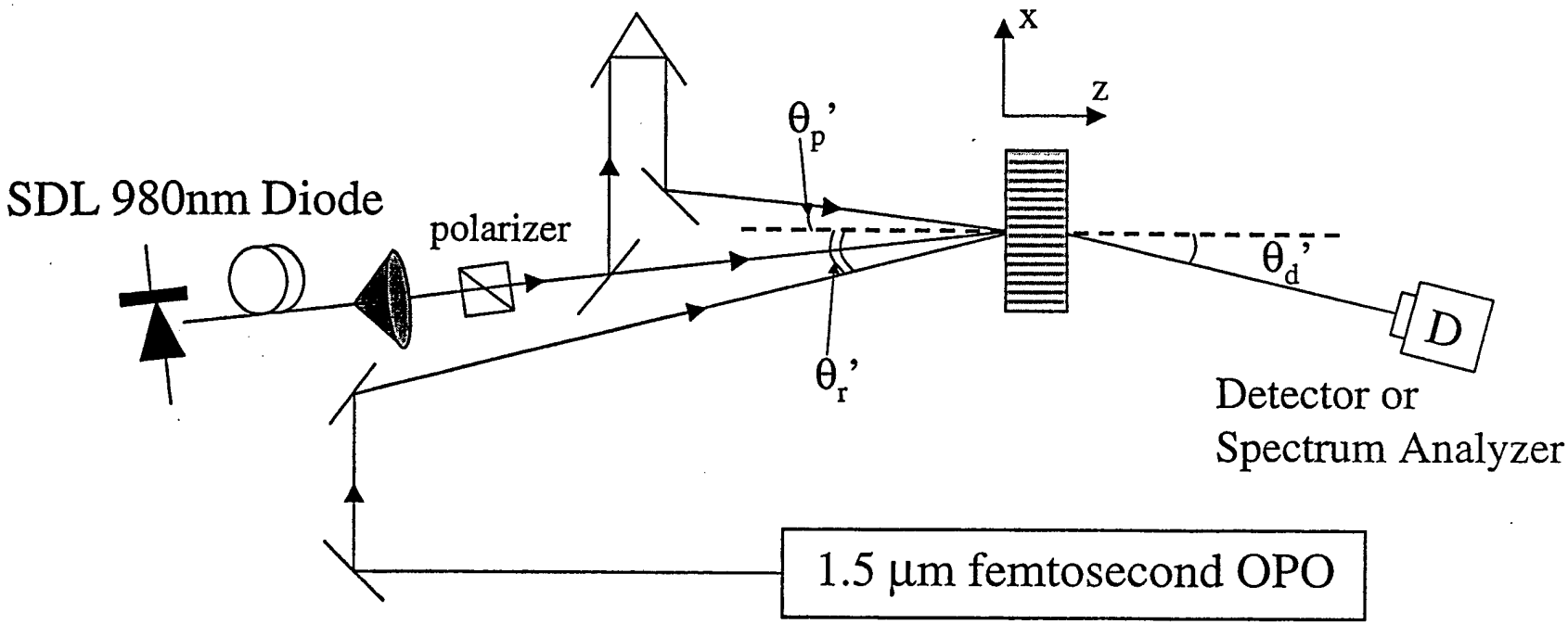
SDL 980nm Diode
polarizer
x
z
θp'
θr'
θd'
D
Detector or
Spectrum Analyzer
1.5 μm femtosecond OPO

Fig. 1

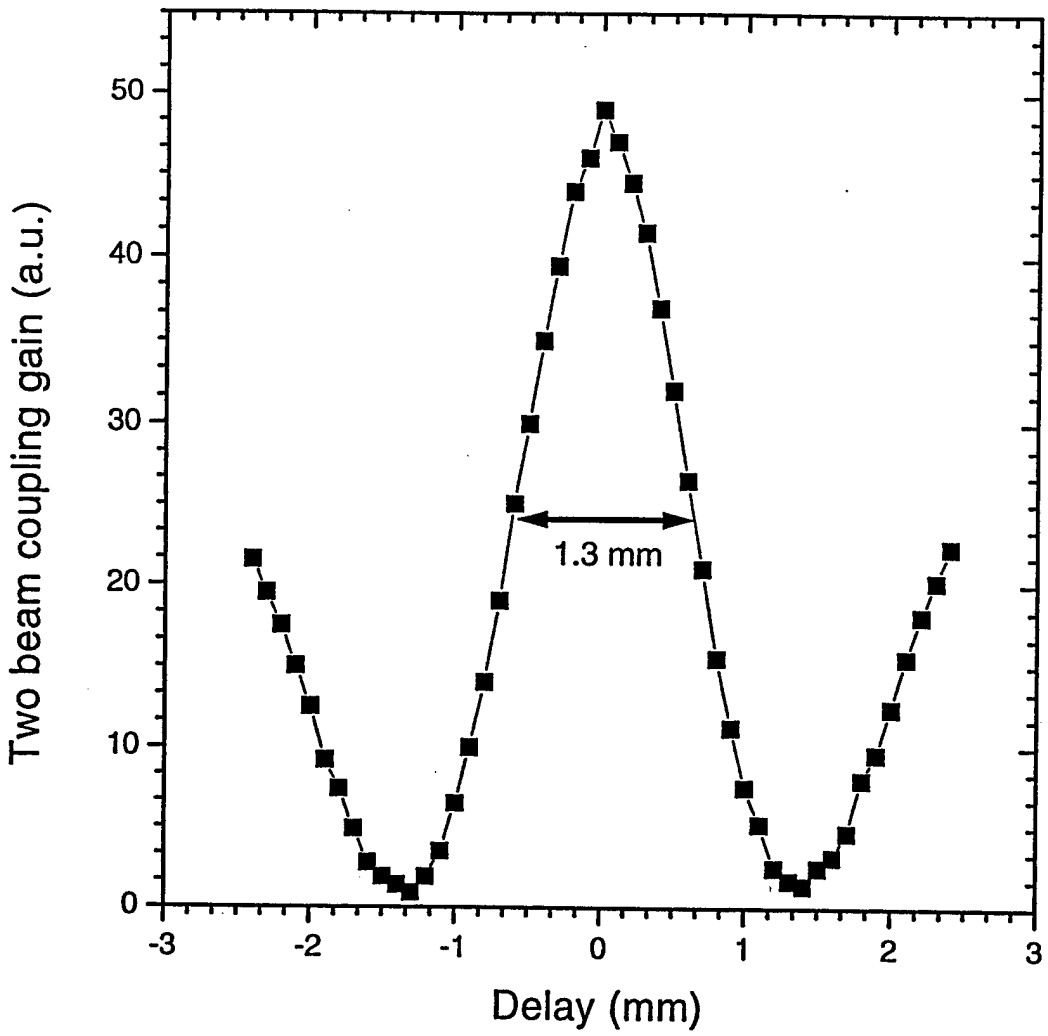
Two beam coupling gain (a.u.)
50
40
30
20
10
0
-3
-2
-1
0
1
2
3
1.3 mm
Delay (mm)

Fig. 2

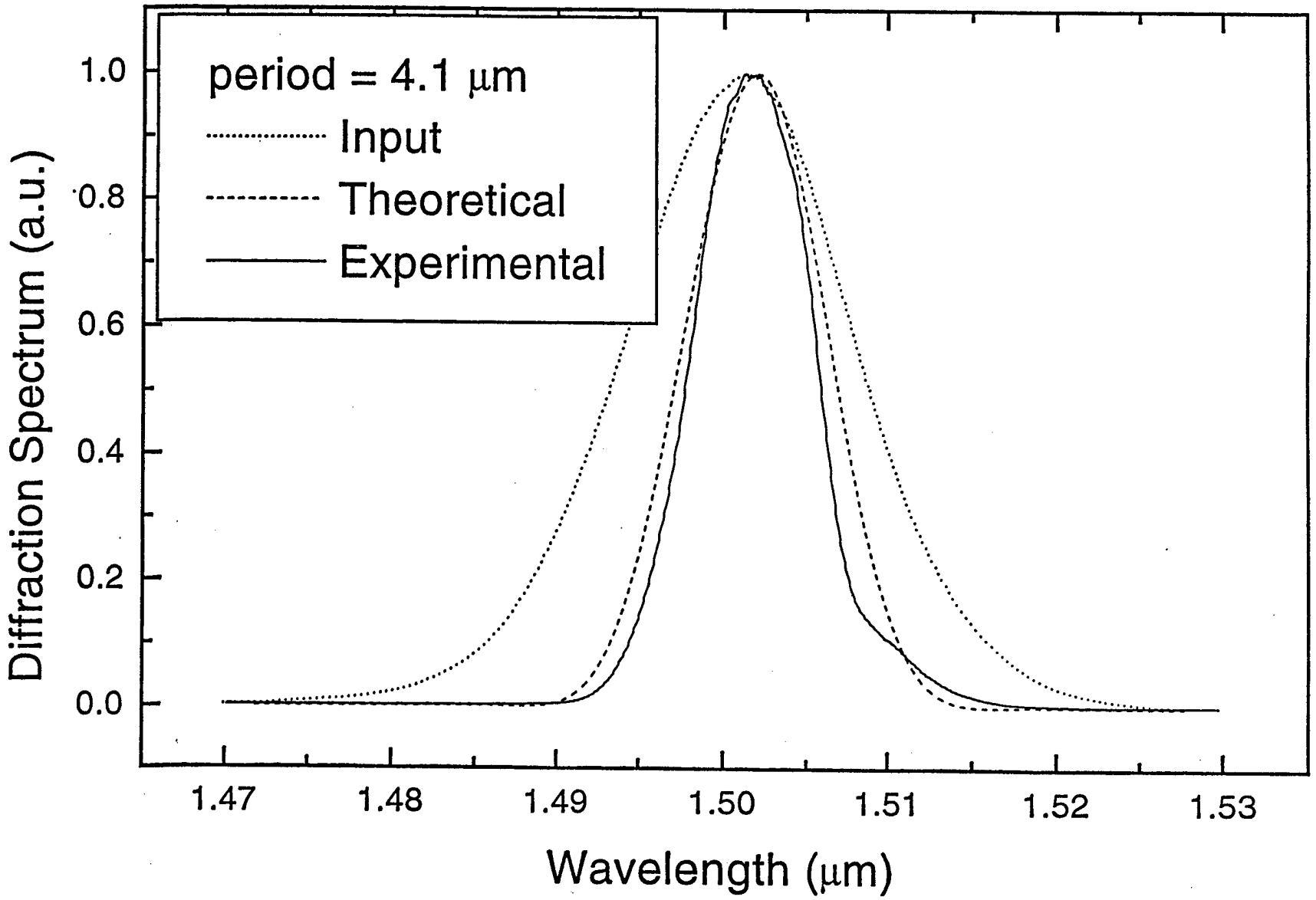
period = 4.1 μm
Input
Theoretical
Experimental
Diffraction Spectrum (a.u.)
1.0
0.8
0.6
0.4
0.2
0.0
1.47
1.48
1.49
1.50
1.51
1.52
1.53
Wavelength (μm)

Fig. 3 (a)

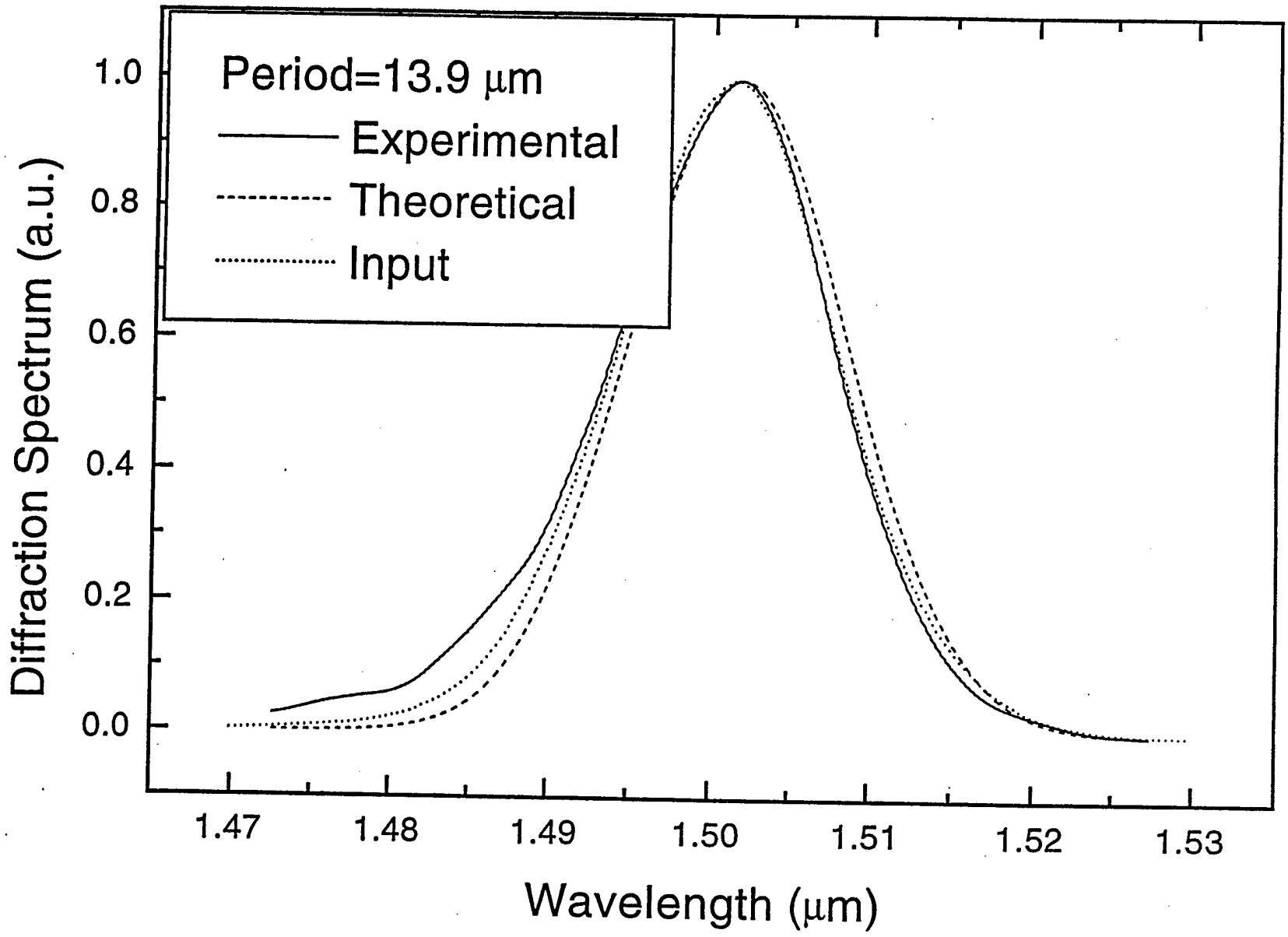
Period=13.9 μm
Experimental
Theoretical
Input
Diffraction Spectrum (a.u.)
1.0
0.8
0.6
0.4
0.2
0.0
1.47
1.48
1.49
1.50
1.51
1.52
1.53
Wavelength (μm)

Fig. 3(b)

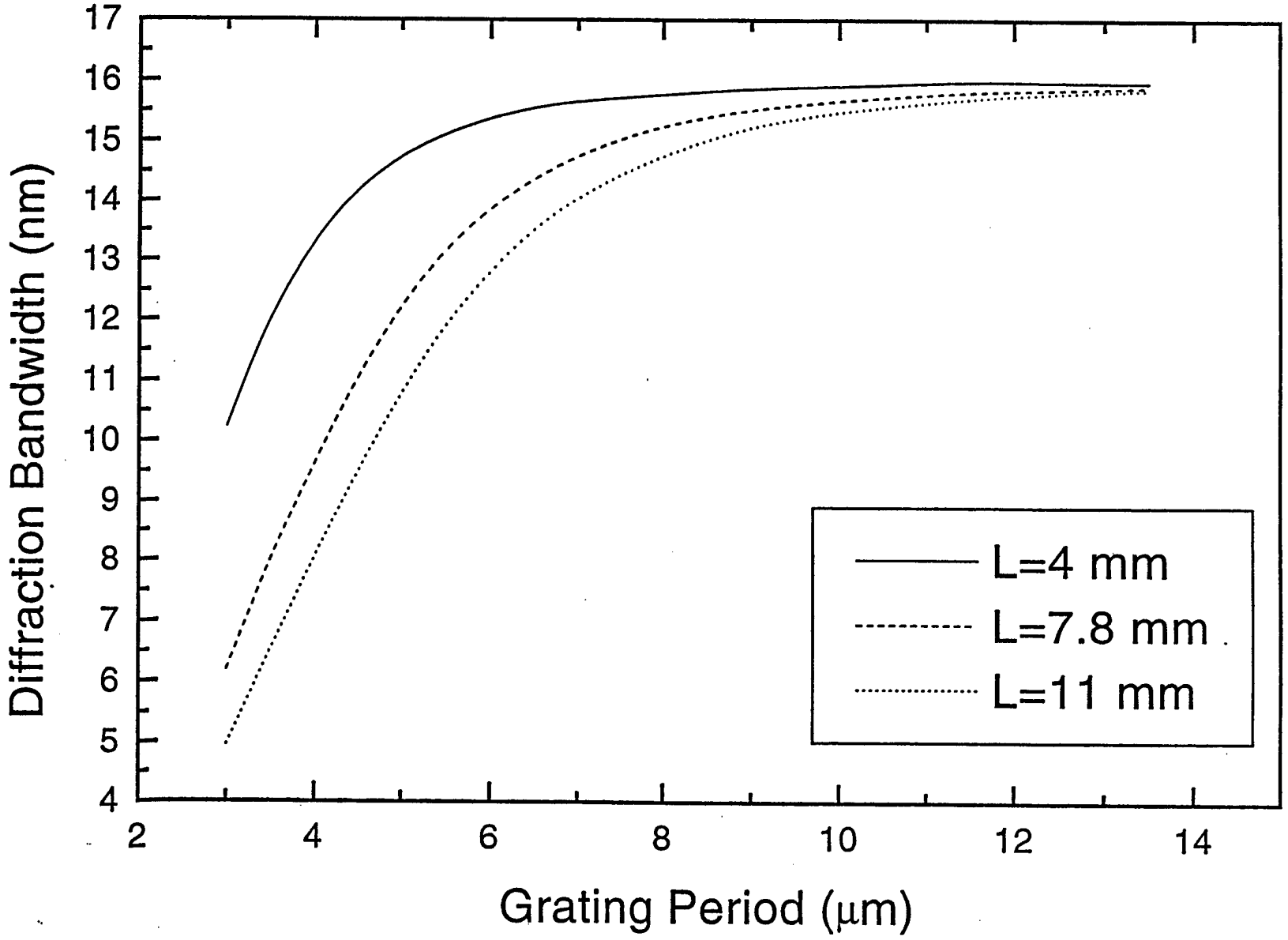
Diffraction Bandwidth (nm)
17
16
15
14
13
12
11
10
9
8
7
6
5
4
2
4
6
8
10
12
14
Grating Period (μm)
L=4 mm
L=7.8 mm
L=11 mm

Fig. 4

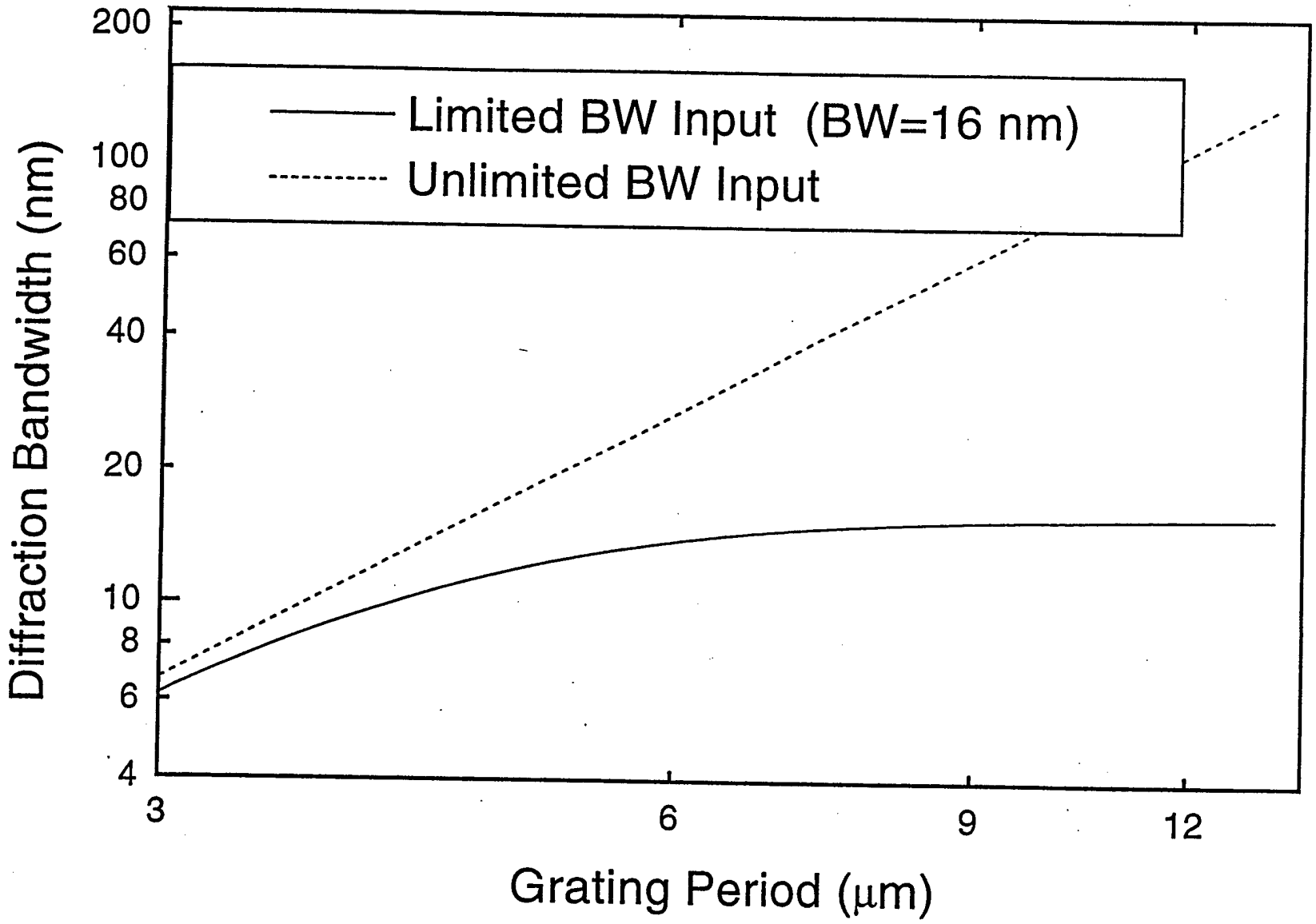
Limited BW Input (BW=16 nm)
Unlimited BW Input
Diffraction Bandwidth (nm)
200
100
80
60
40
20
10
8
6
4
3
6
9
12
Grating Period (μm)

Fig. 5